PAPER • OPEN ACCESS

The effect of Vanadium Addition on the Characteristics of LaCrO$_3$ nanomaterial

View the article online for updates and enhancements.

The effect of Vanadium Addition on the Characteristics of LaCrO$_3$ nanomaterial

Rudy Situmeang[1], Lia Purniasari[1], Harist Oktavian[1] ,Elsina Azmi[1], Simon Sembiring[2]

[1] Department of Chemistry, University of Lampung, Indonesia

[2] Department of Physics, University of Lampung, Indonesia

Abstract. Lanthanum chromite is a material that plays a large role in the development of fuel cells, catalysts, electronic devices, semiconductors, and magnetics. The application of this compound is determined by the material characteristics. The LaCr$_{1-x}$V$_x$O$_3$ (where x = 0.01 – 0.03) compound was prepared using a simultaneous method of sol-gel and freeze-drying from salts of chrome, lanthanum, and vanadium in pectin solution. The characterization results using X-ray diffraction, diffuse-reflectance UV-Vis spectrophotometer, and SEM-EDS. X-ray Diffraction analysis showed that the materials formed have the main structure of ABO$_3$ perovskite (such as LaCrO$_3$ and LaVO$_3$) with minor phases of LaVO$_4$ while the band-gap energy of materials due to the addition of vanadium in LaCrO$_3$, it shifts its energy to a lower direction, namely: 2.7; 2.4; 2.6 eV for LaCr$_{1-x}$V$_x$O$_3$ (where x = 0, 0.01, 0.02, and 0.03) and SEM-EDS micrographs show that the distribution of the crystalline phase is fairly homogeneous, porous and nanorods.

Keywords: Perovskite, nanomaterial, band-gap energy, vanadium

1. Introduction

The choice of advanced material in an application lies in the sensitivity of the conductivity of the material to heat, light, electricity, and other external influences [1] For example, perovskite compounds are very widely used in the fields of fuel cells [2], electricity [3], catalysts [4], refractive materials [5], and semiconductors [6] because of their unique properties. So, understanding the characteristics of a material is the main key in its application.

The perovskite characteristics of LaCrO$_3$ as well as other advanced materials, can be improved by adding M^{2+} or M^{3+} cations (where M = 2nd ionic main group or transition cationic group) both on the La^{3+} site and on the Cr^{3+} site, and even additions to both the La^{3+} and cation sites Cr^{3+} from LaCrO$_3$ perovskite compound. [7].

In the modification of LaCrO$_3$ perovskite compounds prepared through the hydrothermal method, through the addition of the cations. it turns out to provide characteristics of increased conductivity so that it is better to be applied to the reaction [8, 9]. Furthermore, the introduction of M^{n+} dopant into other ABO$_3$ perovskite structures through the sol-gel preparation method turned out to provide suitable characteristics for the photocatalysis process of dyes [10, 11]. Meanwhile, the addition of X^{n+} dopant to other ABO$_3$ advanced materials is also able to increase the characteristics and in line with the improvement in fuel cell performance, [12, 13]. Then choosing the right dopant and proportional amount in modifying an advanced material related to its application becomes the basis for finding the desired advanced material.

On this chance, a study will be reported on the effect of adding vanadium to the LaCrO$_3$ perovskite compound on its characteristics for further application. Due to know the modified LaCrO$_3$ characteristics, analysis techniques such as X-ray diffraction, Diffuse – Reflectance UV-Vis spectroscopy, and SEM-EDS spectroscopy are used to understand the structure, electronic-optical properties, surface morphology of the material and its composition.

2. Materials and Instrumentations

2.1. Materials

Materials that used in this work were pectin powder, $La(NO_3)_3.6H_2O$ (Merck, 99%), $Cr(NO_3)_3.9H_2O$ (Merck, 99%), NH_4VO_3 (Merck, 99%), pyridine (C_5H_5N, J.T Baker), and NH_3 (Merck, 99%), and pectin (domestic market), and distilled water.

2.2. Instrumentations

The characterizations were done using the instruments such as a Philips X-ray diffractometer (XRD) model PW 1710 with Cu-Kα radiation for structural identification, Diffuse Reflectance UV-Vis Spectroscopy (Agilent Cary 60) for measuring band-gap energy and Scanning Electron Microscopy – Electron Dispersive Spectroscopy (SEM - EDS) for identifying grain size distribution, crystallite morphology and composition.

2.3. Preparation of $LaCr_{1-x}V_xO_3$

Stoichiometric amount of Lanthanum (III) nitrate hydrates, Ammonium Vanadate, and Chrome (III) nitrate hydrates were dissolved in distilled water, having compositions $LaCr_{1-x}V_xO_3$ (where x = 0.01 – 0.03) under magnetic stirring for 1 hour, respectively, followed by mixing each solution to make a final solution with weight ratio between nitrates to pectin is 3:2. Adjust the pH=11 in the solution by addition of ammonia, and heat it at 80^oC with continuos stirring to form a viscous gel. Then, dried the gel using freeze dryer for 7 hours to form the precursors' networks and calcined at 600^oC for 3 hours. Finally, V doped $LaCrO_3$ nano photocatalyst obtained.

2.4. Characterization of $LaCr_{1-x}V_xO_3$

2.4.1. X-ray diffractogram analysis.

X-ray powder diffraction pattern of the sample was recorded from $2\Theta = 10$ to 90° on a Philips diffractometer Model PW 1710 using Cu Kα radiation at a step 0.01^o per second. The phase identification was performed using the search and match method by comparing the x-ray pattern of the sample to those of the standards in the JCPDF using Phase Identification from Powder Diffraction Files Window. The particle size was also determined using the Scherrer method [14].

2.4.2. SEM-EDS analysis

To evaluate the surface morphology, the samples were characterized using SEM - EDS. The analysis was conducted on polished and thermally etched samples with different magnifications [15].

2.4.3. Band-Gap energy determination

To determine the band-gap energy of the $LaCr_{0.5}V_{0.5}O_3$ sample, a certain quantity of the sample was analyzed using UV-Vis Diffuse Reflectance Spectroscopy and scanned over the wavelength in the range of 200 – 800 nm.

3. Result and Discussions

3.1. X-ray Diffraction Analysis

The XRD patterns of the samples calcined at 700ºC are collected and treated qualitatively by comparing the diffraction peaks with those of the standard Powder Diffraction Data Base of JCPD files. The search results showed that the crystalline phases formed were $LaCrO_3$ (JCPDF-24-1016) and $LaVO_3$ (JCPDF-11-0024) as dominant and overlapping phases and $LaVO_4$ (25-0427) as minor and impurity phases. The majority of prepared $LaCr_{1-x}V_xO_3$ material forms the perovskite crystalline phases.

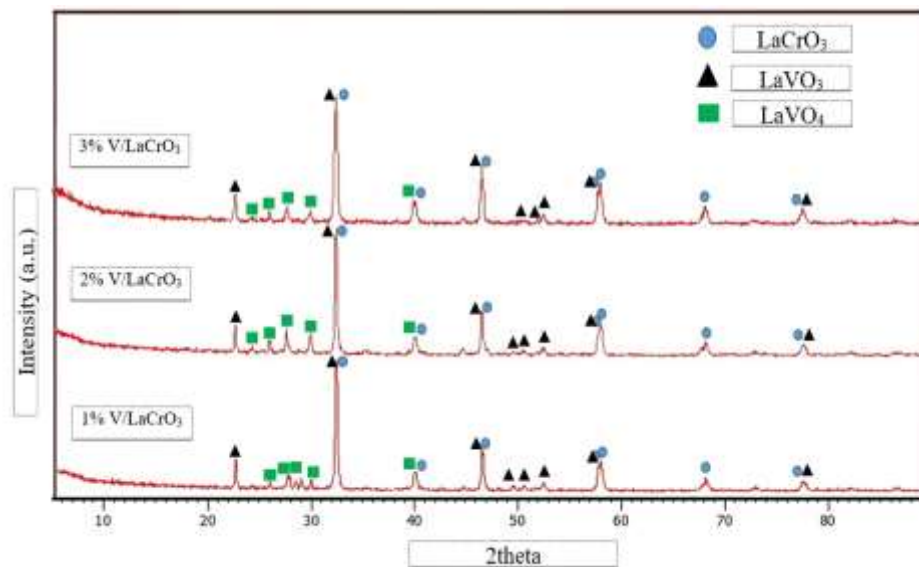**Figure 1.** Difractogram of $LaCr_{0.99}V_{0.01}O_3$, $LaCr_{0.98}V_{0.02}O_3$, and $LaCr_{0.97}V_{0.03}O_3$, respectively.

Furthermore, the size of the crystalline unit cell is determined based on the Scherrer equation [14] and the sizes obtained for $LaCr_{0.99}V_{0.01}O_3$, $LaCr_{0.98}V_{0.02}O_3$, and $LaCr_{0.97}V_{0.03}O_3$ are 80.5; 48.7; and 80 nm.

3.2. Microstructure Analysis

The surface morphology of $LaCr_{1-x}V_xO_3$ (where x = 0.01 − 0.03) material calcined at temperatures of 700 °C was analyzed using SEM as shown in Figure 2. In Figure 2(a), $LaCr_{0.99}V_{0.01}O_3$ has formed a hollow network. The shape of nanorods appears in a part of the surface area, even though it is minor. Furthermore, in Figure 2(b), there are various crystallite sizes formed and cubic, irregular and spherical phases existed. In general, it can be said that there is also a hollow network. In Figure 2(c) it appears that the crystalline phases are fused to form irregular shapes. Furthermore, there is still a hollow network.
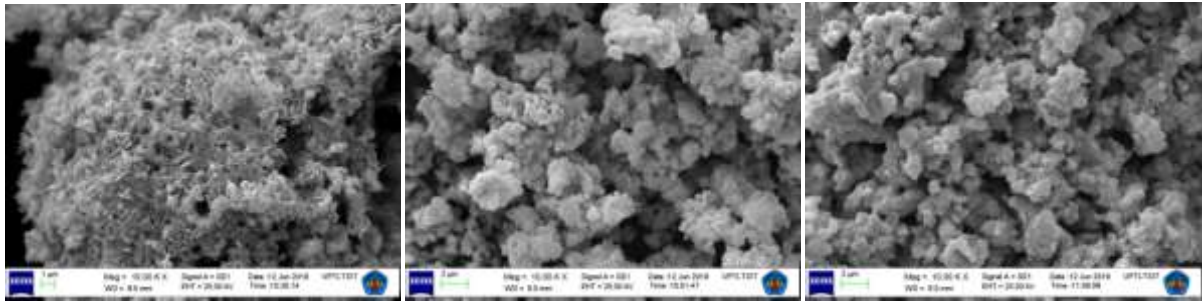
Figure 2. Micrograph of $LaCr_{0.99}V_{0.01}O_3$ (a), $LaCr_{0.98}V_{0.02}O_3$ (b), and $LaCr_{0.97}V_{0.03}O_3$ (c), respectively.

3.3. Band-Gap energy Analysis

Based on a simple analysis using the diffuse - reflectance UV-Vis spectroscopy, the Kubelka-Munk theory [16] and the Tauc [17] plot are used. Mathematically, the Tauc equation is stated as follows:

$$\alpha h\nu = \beta (h\nu - Es)^n \tag{1}$$

where β is a constant, n is an index of values of 1/2, 3/2, 2 or 3 depending on the nature of the electron transition responsible for the absorption. Values of 1/2 or 3/2 referring to a direct transition are allowed or forbidden in a quantum mechanical sense, while those of 2 or 3 correspond to an allowed or a forbidden indirect transition, respectively [34]. The relation between $(\alpha h\nu)^2$ versus $(h\nu)$ plot according to Eq. (1) is shown in Fig. 3 below. The direct optical gap energy can be obtained from the intercept of the resulting straight lines with the energy axis at $(\alpha h\nu)^2 = 0$. The band-gap energy of $LaCr_{1-x}V_xO_3$ (where x = 0.01 − 0.03) prepared at 700°C is 2.7 eV, 2.4 eV, and 2.6 eV, respectively.

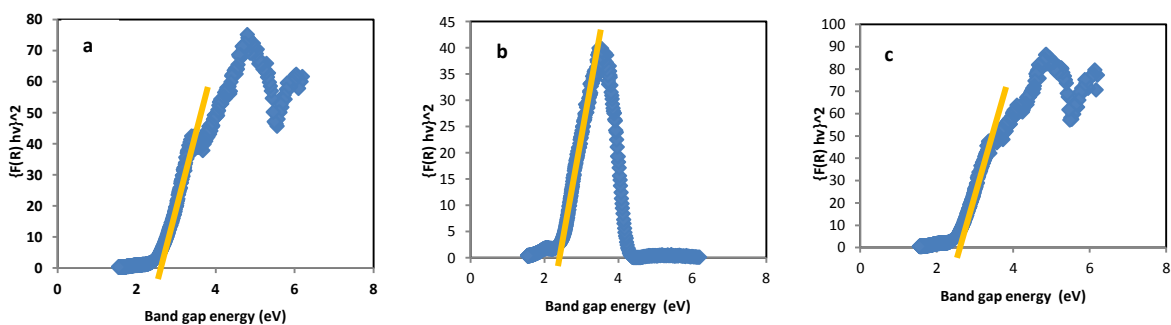**Figure 3.** Bang-Gap energy of $LaCr_{0.99}V_{0.01}O_3$ (a), $LaCr_{0.98}V_{0.02}O_3$ (b), and $LaCr_{0.97}V_{0.03}O_3$ (c), respectively

In general, band gap energy values can be categorized as insulators or semiconductors. If the band gap energy value is e 4.0 eV, it is called an insulator. Meanwhile, if the band gap energy value is e 3.0 eV, it is called a semiconductor [18]. In the prepared $LaCr_{1-x}V_xO_3$ material it can clearly be said to be a semiconductor compound. Furthermore, for photonic applications based on band energy gap it can be said that the prepared material can be used in the UV irradiation range [19, 20].

4. Conclusion

Based on the analysis of $LaCr_{1-x}V_xO_3$ (where x = 0.01 − 0.03) material characteristics, it can be concluded that

1. The prepared materials have the perovskite structure consisting of $LaVO_3$ and $LaCrO_3$,
2. The structure is fairly homogeneous, and has nanorods and porous shapes,

3. Since its band-gap energy below 3.0 eV, this material could be used in photonic applications.

References

[1]. Davis E A 1997 *Endeavor*, New Series vol. 1, no. 314, Pp. 103 – 106
[2]. Yang Y, and You J 2017 *Nature* vol. 554, pp. 155-156.
[3]. Parrey K A, Khandy S A, Laref I I A, Gupta D C, Niazi A, Aziz A, Ansari S G, Khenata R and Rubab S 2018 *J. Electro. Mater.* vol. 47, p. 3615
[4]. Foo G S, Garzon F P, Fung V, Jiang D, Overbury S H and Wu Z 2017 *ACS Catal.* Vol. 7, p. 4423
[5]. Ball J M, Stranks S D, Horantner M T, Huttner S, Zhang W, Crossland E J W, Ramirez I, Riede M, Johnston M B, Friend R H, Snaith H J 2015 Energy *Environ. Sci* vol. 8, no. 2, pp. 602-609.
[6]. Xiao Z, Zhou Y, Hideo H, Kamiya T and Padture N P 2018 *Chem. Eur. J* vol. 24, p. 2305.
[7]. Zhong Z W, and Mi Y 2004 J. *ZheJiang University* vol. 5, no. 12, p. 1471
[8]. Zhang G, Liu G, Wang L, Irvine J T S 2016 *Chem. Soc. Rev.* vol. 45, no. 2, pp. 15951-5984.
[9]. Dong G, Fan H, Tian H, Fang J, Li Q 2015 *RSC Adv.* vol. 5, no. 38, pp. 29618-29623.
[10]. Chen X, and Mao, S S 2007 *Chem. Rev.*, vol. 107, no. 7, pp. 2891–2959.
[11]. Jafry H R, Liga M V, Li Q, and Barron A R 2011 *Environ. Sci. Technol.*, vol. 45, no. 4, pp. 1563–1568.
[12]. Cascos V, Alonso J A, Fernández-Díaz M T 2016 *Materials* vol. *9*, pp. 579 – 591.
[13]. Kobsiriphat W, Madsen B D, Wang Y, Shah M, Marks L D, Barnett S A 2010 *J. Electrochem. Soc.*, vol. *157*, no. *2*, pp. B279-B284.
[14]. Cullity B D 1978 *Elements of X-ray Diffraction*, 2nd ed., Addison-Wesley, London, p. 102.
[15]. Hanke L D 2001 *Handbook of Analytical Methods for Materials*. Materials Evaluation and Engineering Inc. Plymouth, USA, pp. 35 – 38.
[16]. Sangiorgi N, Aversa L, Tatti R, Verucchi R, and Sanson A 2017 *Optical Materials* vol. 64, pp. 18 – 25.
[17]. Liu P, Longo P, Zaslavsky A, and Pacifici D 2016 *J. Appl. Phys.* vol. 119, pp. 014304-1 – 014304-9.
[18]. Urbach F 1953 *J. Phys. Rev.* vol. 92, no. 5, p. 1324.
[19]. Situmeang, R 2019 *Pectins as Emulsifying Agent on the Preparation, Characterization, and Photocatalysis. Book Chapter*. IntechOpen Publisher, England.   DOI: http://dx.doi.org/10.5772/intechopen.83625
[20]. Situmeang R, Sembiring S, Simanjuntak W, Sembiring Z, Yuwono S D 2019 *J. Chem. Techn. Metal.* vol. 54, no. 4, pp. 715-720.